European Radiology (2019) 29:85–92
https://doi.org/10.1007/s00330-018-5531-y

INTERVENTIONAL

Real-time MR-guided brain biopsy using 1.0-T open MRI scanner

Xiangmeng He[1] · Ming Liu[1] · Chao Liu[2] · Jing Fang[3] · Yujun Xu[1] · Ligang Wang[4] · Jianfeng Xiang[5] · Roberto Blanco Sequeiros[6] · Chengli Li[1]

Received: 9 March 2018 / Revised: 24 April 2018 / Accepted: 7 May 2018 / Published online: 12 June 2018

Abstract

Objectives To evaluate the safety, feasibility and diagnostic performance of real-time MR-guided brain biopsy using a 1.0-T open MRI scanner.

Methods Medical records of 86 consecutive participants who underwent brain biopsy under the guidance of a 1.0-T open MRI scanner with real-time and MR fluoroscopy techniques were evaluated retrospectively. All procedures were performed under local anaesthesia and intravenous conscious sedation. Diagnostic yield, diagnostic accuracy, complication rate and procedure duration were assessed. The lesions were divided into two groups according to maximum diameters: ≤ 1.5 cm (n = 16) and > 1.5 cm (n = 70). The two groups were compared using Fisher's exact test.

Results Diagnostic yield and diagnostic accuracy were 95.3% and 94.2%, respectively. The diagnostic yield of lesions ≤ 1.5 cm and > 1.5 cm were 93.8% and 95.7%, respectively. There was no significant difference in diagnostic yield between the two groups (p > 0.05). Mean procedure duration was 41 ± 5 min (range 33–49 min). All biopsy needles were placed with one pass. Complication rate was 3.5% (3/86). Minor complications included three cases of a small amount of haemorrhage. No serious complications were observed.

Conclusions Real-time MR-guided brain biopsy using a 1.0-T open MRI scanner is a safe, feasible and accurate diagnostic technique for pathological diagnosis of brain lesions. The procedure duration is shortened and biopsy work flow is simplified. It could be considered as an alternative for brain biopsy.

Key Points

- *Real-time MRI-guided brain biopsy using a 1.0-T open MRI scanner is safe, feasible and accurate.*
- *No serious complications occurred in real-time MRI-guided brain biopsy.*
- *Procedure duration is shortened and biopsy work flow is simplified.*

Keywords Interventional radiology · Biopsy · Magnetic resonance imaging · Technology · Fluoroscopy

✉ Chengli Li
chenglilichina1966@163.com

[1] Department of Interventional MRI, Shandong Medical Imaging Research Institute affiliated to Shandong University, Shandong Key Laboratory of Advanced Medical Imaging Technologies and Applications, Jinan, Shandong, People's Republic of China

[2] Department of Minimally Invasive Tumor, Tai'an Central Hospital, Tai'an, Shandong, People's Republic of China

[3] Department of Hemodialysis, The Second Affiliated Hospital of Shandong University of Traditional Chinese Medicine, Jinan, Shandong, People's Republic of China

[4] Department of Medical Imaging and Interventional Radiology, Affiliated Yantai Yuhuangding Hospital of Qingdao University, Yantai, Shandong, People's Republic of China

[5] Department of Intervention, Shanghai Jiaotong University Affiliated Sixth People's Hospital South Campus, Shanghai, People's Republic of China

[6] South Western Finland Imaging Centre, Turku University Hospital, Turku, Finland

Abbreviations

NeuroICU	Neuro intensive care unit
RF	Radiofrequency
T1W-TSE	T1-weighted turbo spin echo
T2W-TSE	T2-weighted turbo spin echo

Introduction

Accurate diagnosis of brain lesions is an important prerequisite for optimised treatment. Although modern imaging provides ample information for diagnosis, it cannot replace the crucial role of biopsy and histopathological diagnosis, especially in suspected malignancy. At present, there are three major types of surgical procedures for brain biopsy: frame-based, frameless and intraoperative MRI-guided brain biopsy. Although frame-based stereotactic brain biopsy has been the most commonly used method with good diagnostic performance, there are limitations to this technique, the main one being the absence of real-time image feedback during biopsy procedure [1]. During operation, the accurate location of needle and biopsy target cannot be visualised, which may lead to false negative results and intraoperative morbidity [2–5]. Real-time MRI-guided brain biopsy overcomes this limitation and has been applied increasingly in recent years. Although this technique provides high diagnostic yield and lower rate of serious complications [6], the biopsy procedure requires auxiliary apparatus [7, 8]; and the procedure is complicated leading to longer procedure times [7]. In addition, most of the reported procedures were performed using a closed-bore MR scanner without a larger open access. In closed-bore scanners, the patient access can be restricted to some extent [8]. Although low-field magnets have larger open access, the signal-to-noise ratio is lower for biopsy guidance, which may limit its application in brain biopsy. Open high-field MR scanners with large open space and better imaging are expected to feasible for biopsy guidance.

In our study, we used a 1.0-T open interventional MR scanner, with large 160-cm left-to-right and 40-cm anteroposterior apertures, and real-time technique for brain biopsy. Real-time and MR fluoroscopy techniques in 1.0-T open MR have been utilised in guidance of biopsy procedures and interventional therapy, such as liver biopsy, radiofrequency ablation, periradicular injection therapy, etc. [9–13]. Recent studies have shown that real-time technique in 1.0-T open MR provides a time-efficient, simplified and accurate approach for biopsy guidance with clinical value [9, 10]. However, to the best of our knowledge, 1.0-T open MR has not been used in brain biopsy procedures thus far.

The aim of this study was to evaluate the safety, feasibility and diagnostic performance of applying a 1.0-T open MRI scanner with real-time and MR fluoroscopy techniques in brain biopsy.

Material and methods

Patients

We selected a retrospective cohort from our medical record system between July 2014 and February 2017. During the time frame indicated, 86 consecutive patients (46 male, 40 female) with intracerebral lesions were biopsied using a 1.0-T open MRI scanner in our institution. Thirty-three of the 86 patients underwent surgical resection subsequently. Patient demographics, imaging data, surgical characteristics and histopathological diagnosis were retrospectively reviewed. All patients had intracranial mass lesions shown by CT or MR images. The 86 intracerebral lesions were divided into two groups according to their maximum diameters: lesions ≤ 1.5 cm (n = 16) and lesions > 1.5 cm (n = 70).

This study plan was approved by the institutional review board of Shandong University.

Equipment and technique

Real-time MRI-guided brain biopsies were carried out with a 1.0-T open MRI scanner (Philips Healthcare, Amsterdam, Netherlands). An out-of-room console and an in-room MR-compatible radiofrequency (RF)-shielded liquid crystal monitor (Philips Healthcare, Amsterdam, Netherlands), which was placed near to the magnet, were used to display images and guide biopsy procedure. The suite was equipped with an MR-compatible electrocardiogram monitor. A high-speed drill was used to penetrate the skull. An MR-compatible coaxial needle with a blunt tip (16-G, Wanlin Medical, Qingdao, Shandong, China) and a semi-automated biopsy needle (18G, TSK TM, TSK Laboratory, Tochigi-shi, Japan) were used to obtain specimens. All biopsy procedures were performed by the same two experienced interventional radiologists.

Preoperative preparation

Patients were placed on the operating table of the MR scanner in a suitable position, which was determined by lesion accessibility. The position of the patient was fixed by a vacuum bag. A receive-type flexible surface loop coil with the diameter of 30 cm was wrapped around the patient's head close to the area of interest. An MRI-compatible electrocardiogram monitor was used to monitor vital signs, including cardiac rhythm, oxygen saturation and blood pressure. Haemostasis was maintained with ethamsylate (2.0 g) to prevent bleeding in the biopsy procedure. Intravenous administration of gadolinium-DTPA (0.2 ml/kg) was used for contrast enhancement.

Biopsy procedure

A fish oil capsule marker was placed on the surface of the scalp before preoperative imaging. Then the patient underwent enhanced MR imaging. Enhanced images of T1-weighted turbo spin echo (T1W-TSE) (TR 447 ms, TE 10 ms, flip angle 90°, slice thickness/separation 5 mm/1 mm, matrix 240 × 165, FOV 230 × 199) and T2-weighted turbo spin echo (T2W-TSE) (TR 2494 ms, TE 107 ms, flip angle 90°, slice thickness/separation 5 mm/1 mm, matrix 240 × 158, FOV 230 × 199) were used to confirm the target lesion. The fish oil capsule marker and the target point were used to define the arbitrarily angulated plane to display the entry point and the lesion in one image. The puncture trajectory was determined to avoid eloquent areas, large arteries and veins. According to puncture trajectory, the approach angle and the distance from the skin to the lesion were measured. Then the patient was moved outside of the magnet bore and given local anaesthesia using lidocaine (2%, 2.5 mL) and intravenous conscious sedation using diazepam (5 mg). A twist-drill hole was made at the entry point by an interventional radiologist using a battery-operated twist drill (3.5 mm diameter). Then the patient was moved back into the magnet. On the real-time interface, the puncture process was guided by MR fluoroscopy with continuous real-time imaging (Figs. 1 and 2). Real-time MRI sequences included T1W gradient echo sequence (T1W-FFE), T1W-TSE sequence and T2W-TSE sequence (Table 1). The highest image frame rate was 1 image per 2.9 s. Selection of the sequence was determined by the enhancement features of the lesion. The interactive dynamic viewing of needle orientation and position could be displayed in two adjustable orthogonal image planes on the monitor in the operating room (Fig. 3). Needle orientation was adjusted if it was necessary according to the continuous imaging until the needle punctured the target. Then the patient was moved outside of the magnet bore again and the sampling procedure was performed with an 18-G semi-automated cutting needle. Three to five specimens were collected from different quadrants of each lesion for histopathological examination. Immunohistochemical analysis was performed as required.

Post-procedure evaluation

After the needle withdrawal, the patient was moved back into the magnet and a final set of images of the entire brain was obtained. By comparing with the preoperative imaging, we observed whether any complications occurred. If haemorrhage was detected, the amount of bleeding was estimated. The procedure duration, the number of needle passes and postoperative complications were recorded. The time from patient positioning to the removal of the needle was defined as the total procedure duration. One puncture trajectory was defined as one needle pass. After the biopsy procedure, patients continued to be monitored in hospital and were not transferred to the neuro intensive care unit (NeuroICU) for observation; mannitol and haemostatic drugs were administered to patients for 2–3 days. Postoperative MRI was achieved routinely 1 day after biopsy procedure to assess any delayed intracranial bleeding. A small amount of haemorrhage was treated with conservative treatment, but any severe symptomatic haemorrhage after biopsy was treated with surgical evacuation by craniotomy.

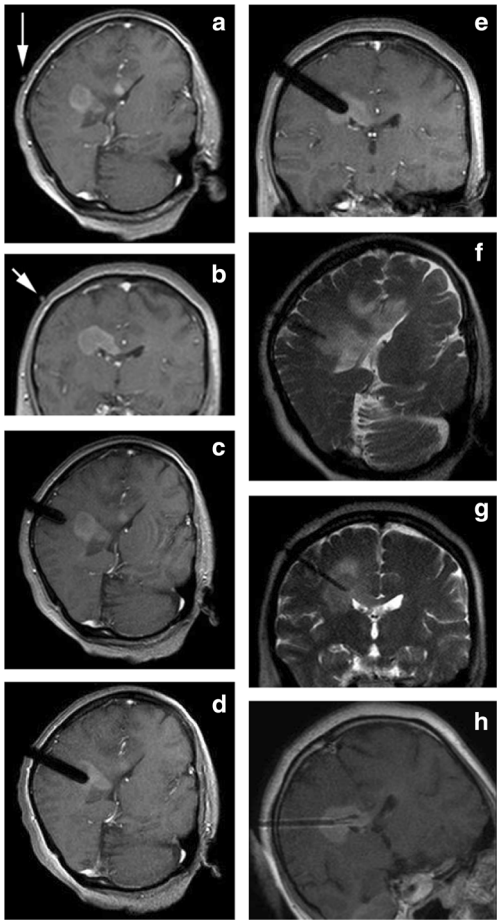

Fig. 1 A 60-year-old woman underwent real-time MRI-guided brain biopsy. **a**, **b** Preoperative T1W contrast-enhanced MR images for determination of the entry point and the puncture trajectory. Fish oil capsule (arrow) was placed on the surface of skull to determine the entry point. **c**–**e** T1W-FFE images of real-time MRI-guided puncture procedure. The needle was displayed continuously in real time until it punctured the lesion. **f**, **g** T2W-TSE images from the puncture procedure. **h** T1W MR image after the biopsy procedure. Specimens were obtained from the areas of the lesion which were displayed in T1W MR image. The biopsy specimen revealed an anaplastic astrocytoma

Statistical analysis

Histopathology results were recorded. The diagnostic yield and complication rate were calculated. The diagnostic accuracy was calculated by comparing biopsy histopathological diagnoses with final diagnoses obtained by surgery or clinical follow-up of a mean of 14 months (range 12–24 months) after brain biopsies. Two-tailed Fisher's exact test was used to

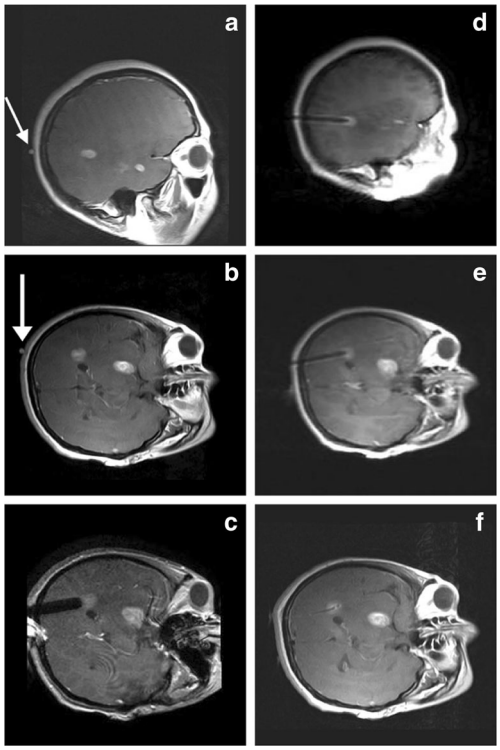

Fig. 2 A 37-year-old woman underwent real-time MRI-guided brain biopsy. **a**, **b** Contrast-enhanced MR images before the puncture procedure. Fish oil capsule (arrow) was placed on the surface of the skull to determine the entry point. **c** Enhanced T1W-FFE image from real-time MRI-guided puncture procedure. The needle was displayed continuously in real time until it punctured the lesion. **d**, **e** The position of the needle tip was reconfirmed by sagittal and transverse images of real-time T1W-TSE. **f** T1W MR image after biopsy procedure. Specimens were obtained from the areas of the lesion displayed in T1W MR image. The biopsy specimen revealed a neurosarcoidosis

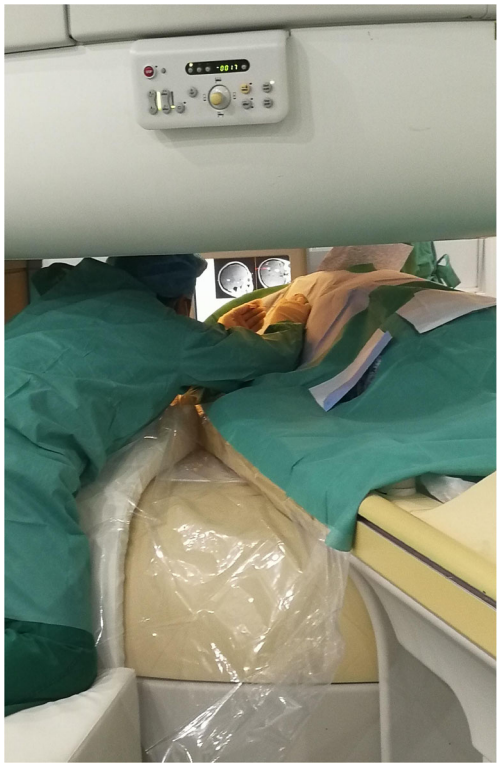

Fig. 3 1.0-T open interventional magnetic resonance system. The operator holds the needle and punctures the target under the guidance of real-time MRI; images are displayed on the removable RF-shielded liquid crystal monitor in front of the operator

compare diagnostic yield in two groups (maximum diameter ≤ 1.5 cm, maximum diameter > 1.5 cm). Statistics analysis was performed by SPSS 22.0 statistical software. *P* values less than 0.05 were considered to indicate significant differences.

Results

In 86 patients with undefined intracranial lesions, 86 brain biopsies were performed. Mean patient age was 52 years (range 12–76 years). Mean maximum diameter of the lesion was 2.1 ± 0.8 cm (range 0.9–4.1 cm). Procedure duration was 41 ± 5 min (range 33–49 min). All biopsy needles were placed with one pass.

All biopsy specimens were technically successfully obtained. Eighty-two procedures yielded definitive diagnoses in all 86 procedures (Table 2). Diagnostic yield was 95.3% (82/86). There were four non-definitive histopathological results, including two cases of atypical cells and two cases of gliosis. The diagnostic yield of lesions ≤ 1.5 cm and > 1.5 cm were 93.8% (15/16) and 95.7% (67/70), respectively. There was no significant difference in diagnostic yield between the two groups; $p > 0.05$ by Fisher's exact test (Table 3).

The final diagnoses of 31 cases with definitive histopathological diagnoses and 2 cases with non-definitive histopathological diagnoses at needle biopsy were obtained by subsequent surgical resection; the final diagnoses of 53 cases were obtained by clinical follow-up. The final diagnoses results confirmed the biopsy results in 81 patients with diagnostic accuracy of 94.2% (81/86) (Table 2). Two cases thought to be anaplastic astrocytoma after needle biopsy were confirmed to be higher grade tumour (glioblastoma multiforme). One false negative case diagnosed as demyelinating lesion after needle biopsy was confirmed to be lymphoma by cytological examination of cerebrospinal fluid. The other two false negative cases diagnosed as atypical cells were confirmed as lymphoma and anaplastic astrocytoma, respectively, by subsequent surgery.

No serious complications occurred. Minor complications included three cases of a small amount of haemorrhage in the biopsy procedure, including one case of epidural haemorrhage and two cases of cerebral haemorrhage. The amount of bleeding was about 2.3 ml, 0.6 ml and 0.5 ml, respectively. MRI revealed no increase in bleeding 24 h after operation. All three patients had no obvious clinical symptoms after drug treatments (mannitol and haemostatics) for 3–7 days. The complication rate was 3.5% (3/86).

Table 1 Parameters of real-time MRI sequences

Sequence	TR (ms)	TE (ms)	Flip angle (degree)	Slice thickness (mm)	Matrix	FOV	Acquisition time (s)
T1W-FFE	25	6.91	30	6	140 × 111	180 × 144	2.9
T1W-TSE	300	6.2	90	8	128 × 110	180 × 180	7.5
T2W-TSE	2500	108	90	5	256 × 154	230 × 183	2

T1W-FFE T1-weighted gradient echo, *T1W-TSE* T1-weighted turbo spin echo, *T2W-TSE* T2-weighted turbo spin echo, *TR* repetition time, *TE* echo time, *FOV* field of view

Discussion

In our study, the diagnostic yield was 95.3% and diagnostic accuracy was 94.2%, showing good performance for stereotactic brain biopsy and were comparable with the data in reported literature: the diagnostic yield in reported studies on stereotactic brain biopsy ranges between 82.1% and 99.3% [6, 14–18]; the diagnostic accuracy ranges between 80% and 96.7% [2, 19, 20]. In these studies, frame-based and frameless stereotactic brain biopsies are the main operative methods; real-time MR technique was not widely used. There are some drawbacks of the two techniques of stereotactic brain biopsy. When performing brain biopsy using frame-based and most frameless stereotactic techniques without imaging feedback, preoperative images are used to access target tissue; therefore, there are no intraoperative images confirming the location of the needle, which may lead to deviation of the needle trajectory and inaccurate sampling. It may also lead to serious or fatal complications, such as neurologic deficit and fatal haemorrhage [2–5, 21]. In our study, the real-time guided puncture process allowed the operator to detect the intraoperative brain shift in time and to compensate for the deviation, which is identified as a possible cause leading to an inaccuracy diagnosis [22]. Grunert et al. [23] used a frameless system with optical navigation to guide the

Table 2 Outcome of real-time MR-guided brain biopsy (n = 86)

Histopathologic finding	Needle biopsy	Follow-up					Consistent [a]
		Resection	Clinical				
			Con	C or R	M	O	
Glioma	45	27	1	17			43
Glioblastoma multiforme (IV)	19	13		6			19
Anaplastic astrocytoma (III)	9	5		4			7
Anaplastic oligoastrocytoma (III)	4	2		2			4
Astrocytoma (II)	8	2	1	5			8
Oligodendroglioma (II)	3	3					3
Oligoastrocytoma (II)	2	2					2
Ependymoma	2	0		2			2
Primitive neuroectodermal tumour (IV)	2	2					2
Lymphoma	10	0		10			10
Metastasis	7	2		5			7
Benign lesions	16	0			15	1	15
Demyelinating lesion	8	0			8		7
Abscess	2	0			2		2
Radiation necrosis	1	0				1	1
Neurosarcoidosis	2	0			2		2
Encephalitis	3	0			3		3
Non-definitive diagnosis	4	2				2	2
Atypical cells	2	2					0
Gliosis	2	0				2	2
Total	86	33	53				81

Con conservative management, *C* chemotherapy, *R* radiation therapy, *M* medicine, *O* observation

[a] Histopathologic diagnoses obtained by needle biopsy with final diagnoses obtained by surgical resection and clinical follow-up

Table 3 Results of each group based on the lesion size

Maximum lesion diameter	Patients (*n*)	Definitive (*n*)	Not definitive (*n*)	Diagnostic yield (%)	*p** value
≤ 1.5 cm	16	15	1	93.8% (15/16)	0.568
> 1.5 cm	70	67	3	95.7% (67/70)	

*Fisher's exact test

brain biopsy and came to the conclusion that the frameless system was effective for performing brain biopsies of relatively large lesions (> 1.5 cm). Our study indicated that, for lesions with diameter < 1.5 cm, the diagnostic yield of the lesion was comparable to that of lesions with diameter > 1.5 cm (Table 3). We concluded that the precise guidance of the real-time technique and the multiparametric sequences clearly showing the target and the needle simultaneously may have contributed to this result. In our biopsy process, we were capable of visualising the target lesion and needle position in two orthogonal MR image planes (such as transverse and coronal planes) in real time, which helped the operator to keep the needle in the right direction until the needle was advanced into the target.

The four non-definitive histopathological diagnoses included two cases of atypical cells and two cases of gliosis. Two of the four cases had bleeding from the lesion in the biopsy process, resulting in inadequate specimens and false negative outcomes. Both of the other two patients with diagnoses of gliosis had a history of previous chemoradiotherapy with temozolomide. They were diagnosed with pseudoprogression by follow-up for 18 months. Other researchers reported the same difficulty of confirming the histopathological diagnoses in patients with a history of radiotherapy [6, 24]. The third false-negative case with diagnosis of demyelinating lesion was confirmed to be lymphoma. We consider that the heterogeneity of the tumour may have led to the inaccurate result. It was found that neoplastic cells in lymphoid neoplasms can be admixed with reactive brain elements, degenerative and inflammatory elements [25].

For the biopsy procedure, we used MR fluoroscopy technique to guide the puncture process. Real-time MR displays the needle trajectory in two orthogonal planes, which can be alternated repeatedly and rapidly. The image frame rate was 2.9 s per image. When it was necessary, the operator could adjust the needle orientation easily and rapidly in an interactive mode, without stopping the MR scanning and consequently repetitively moving the patient out and back into the MRI bore. The procedure duration was efficient. In our cases, the average procedure duration was 41 ± 5 min (range 33–49 min), which was much shorter than that reported in earlier studies [7, 26, 27]. Gempt et al. [27] used frameless MR-guided stereotaxy for brain biopsy. Mean patient time in the operating room, including navigation registration, patient positioning and operation, was 99 ± 28 min (range 49–189 min). Mohyeldin et al. [7] used real-time MRI in the guidance of brain biopsy. Mean operative time was 114 ± 42.8 min. Our significantly shorter procedure duration was not only attributed to our rapid imaging speed and real-time technique but also to their unnecessary installation of fixation and navigation apparatus. Additionally, the application of local anaesthesia also shortened the operation time. In our study, we found that local anaesthesia in brain biopsy is feasible and safe. The shortened operation time and application of local anaesthesia had some benefits. Firstly, as the biopsy duration is short, the influence of the time-dependent washout of contrast media is minimised. Secondly, the medical costs can be reduced.

As the interactive imaging platform simplifies the workflow of the biopsy procedure, there is no need for the apparatus that was formerly used, such as frames, rigid instrument holder, neuro-navigator or optical tracking sensor. The puncture needle has a large adjustment space and, should there be any unwanted head movement, the needle can be visualised before entering the dura and adjusted to the correct trajectory. As a result there was no need for the skull-mounted aiming device typically used in brain biopsy. As a whole, the real-time MRI-guided brain biopsy can be seen to possibly reduce discomfort caused by an ordinary patient frame's bulkiness and the risk of infection at the frame's fixture points.

The complication rate in our study was 3.5% and no serious complications occurred. For frame-based and frameless stereotactic brain biopsy, complication rates are reported to range from 3% to 12%, with an average mortality rate of 1.1% [14, 19, 28–30]. The complication rate in our study was in the expected range and, more importantly, there were no severe complications. As the image feedback was all in real time, minor changes in the position of the patient or brain shift could be detected in time, and the route of the puncture needle could be adjusted in time if necessary. Hence, all patients were punctured with one pass. It has been reported that multiple puncture passes are associated with the presence of postoperative haemorrhage [16]. Woodworth et al. [21] reported that cortical biopsy samplings needed additional needle passes in 11% of biopsy procedures when performing frame-based brain biopsy. In our study, we did not observe any increase in needle passes due to inaccurate puncture execution; this may have contributed to decreased complications in our study.

The selection of MRI sequences for puncturing guidance was determined according to the lesion features. T1W-FFE, T1W-TSE and T2W-TSE sequences were used in biopsy procedure with different acquisition time and size of the susceptibility artefact of the needle. The acquisition time of T1W-

FFE sequence is the shortest and the artefact of the needle is the largest. The T1W-TSE sequence is not as fast as the T1W-FFE sequence, but the size of the needle artefact is optimal. The T1W-FFE sequence is a better choice for guiding biopsy procedure of relatively large lesions in order to shorten operation time. The T1W-TSE sequence was adopted for biopsy guidance of smaller targets, as T1W-TSE imaging was better for displaying the accurate distance between the needle and lesion with better image quality and optimal needle artefact. If the lesion did not enhance with contrast, the T2W-TSE sequence was chosen.

A number of studies have been carried out using high-field magnetic resonance imaging to guide brain biopsy [7, 8]. Hall et al. [8] used a 1.5-T MRI system for brain biopsy and showed its effectiveness for evaluating lesions of the brain. However, as a result of the limitation of the scanner bore opening, the patient's position in the biopsy procedure was limited. For example, the lateral position could not be adopted. Open magnetic resonance scanners allow more free-positioning which favours the biopsy procedure. Another advantage of the open magnet is that it allows the operator to be close to the patient. It is beneficial for the operator to observe any patient discomfort and to reduce the patient's stress during the biopsy process. The local anaesthesia contributes to patient safety by enabling the patients' cognition to be monitored during the procedure.

Our study has at least two limitations. First, the retrospective design may result in case selection bias. Second, we did not have comparative studies concerning the diagnostic performance, complication rate and procedure duration with frame-based stereotactic brain biopsy.

In summary, real-time MR-guided brain biopsy with MR fluoroscopy using a 1.0-T open MRI scanner is a safe, feasible and accurate diagnostic technique for pathological diagnosis of brain lesions. It could simplify biopsy workflow and shorten procedure duration and could be considered as an alternative for brain biopsy.

Funding This study has received funding by Shandong Science and technology development plan (2014GGH218005).

Compliance with ethical standards

Guarantor The scientific guarantor of this publication is Chengli Li.

Conflict of interest The authors of this manuscript declare no relationships with any companies whose products or services may be related to the subject matter of the article.

Statistics and biometry All authors kindly provided statistical advice for this manuscript.

No complex statistical methods were necessary for this paper.

Informed consent Written informed consent was obtained from all subjects (patients) in this study.

Ethical approval Institutional review board approval was obtained.

Methodology
- retrospective
- diagnostic or prognostic study
- performed at one institution

References

1. Ivan ME, Yarlagadda J, Saxena AP et al (2014) Brain shift during bur hole-based procedures using interventioanl MRI. J Neurosurg 121:149–160
2. Ersahin M, Karaaslan N, Gurbuz MS et al (2011) The safety and diagnostic value of frame-based and CT-guided stereotactic brain biopsy technique. Turk Neurosurg 21:582–590
3. Lobão CA, Nogueira J, Souto AA, Oliveira JA (2009) Cerebral biopsy: comparison between frame-based stereotaxy and neuronavigation in an oncology center. Arq Neuropsiquiatr 67: 876–881
4. Hall WA (1998) The safety and efficacy of stereotactic biopsy for intracranial lesions. Cancer 82:1749–1755
5. Nishihara M, Sasayama T, Kudo H, Kohmura E (2011) Morbidity of stereotactic biopsy for intracranial lesions. Kobe J Med Sci 56: E148–E153
6. Lu Y, Yeung C, Radmanesh A, Wiemann R, Black PM, Golby AJ (2015) Comparative effectiveness of frame-based, frameless, and intraoperative magnetic resonance imaging–guided brain biopsy techniques. World Neurosurgery 83:261–268
7. Mohyeldin A, Lonser RR, Elder JB (2016) Real-time magnetic resonance imaging-guided frameless stereotactic brain biopsy: technical note. J Neurosurg 124:1039–1046
8. Hall WA, Martin AJ, Liu H, Nussbaum ES, Maxwell RE, Truwit CL (1999) Brain biopsy using high-field strength interventional magnetic resonance imaging. Neurosurgery 44:807–813
9. Fischbach F, Bunke J, Thormann M et al (2011) MR-guided freehand biopsy of liver lesions with fast continuous imaging using a 1.0-T open MRI scanner: experience in 50 patients. Cardiovasc Intervent Radiol 34:188–192
10. Fischbach F, Eggemann H, Bunke J, Wonneberger U, Ricke J, Strach K (2012) MR-guided freehand biopsy of breast lesions in a 1.0-T open MR imager with a near-real-time interactive platform: preliminary experience. Radiology 265:359–370
11. Streitparth F, Walter T, Wonneberger U et al (2014) MR guidance and thermometry of percutaneous laser disc decompression in open MRI: an ex vivo study. Cardiovasc Intervent Radiol 37:777–783
12. Maurer MH, Disch AC, Hartwig T et al (2014) Outcome study of real-time MR-guided cervical periradicular injection therapy in an open 1.0 Tesla MRI system. Cardiovasc Intervent Radiol 37:756–762
13. Fischbach F, Lohfink K, Gaffke G et al (2013) Magnetic resonance-guided freehand radiofrequency ablation of malignant liver lesions: a new simplified and time-efficient approach using an interactive open magnetic resonance scan platform and hepatocyte-specific contrast agent. Invest Radiol 48:422–428
14. McGirt MJ, Woodworth GF, Coon AL et al (2005) Independent predictors of morbidity after image-guided stereotactic brain biopsy: a risk assessment of 270 cases. J Neurosurg 102:897–901
15. Paleologos TS, Dorward NL, Wadley JP, Thomas DG (2001) Clinical validation of true frameless stereotactic biopsy: analysis of the first 125 consecutive cases. Neurosurgery 49:830–837
16. Air EL, Leach JL, Warnick RE, McPherson CM (2009) Comparing the risks of frameless stereotactic biopsy in eloquent and

noneloquent regions of the brain: a retrospective review of 284 cases. J Neurosurg 111:820–824
17. Shooman D, Belli A, Grundy PL (2010) Image-guided frameless stereotactic biopsy without intraoperative neuropathological examination. J Neurosurg 113:170–178
18. Dammers R, Schouten JW, Haitsma IK, Vincent AJ, Kros JM, Dirven CM (2010) Towards improving the safety and diagnostic yield of stereotactic biopsy in a single center. Acta Neurochir (Wien) 152:1915–1921
19. Owen CM, Linskey ME (2009) Frame-based stereotaxy in a frameless era: current capabilities, relative role, and the positive and negative predictive values of blood through the needle. J Neurooncol 93:139–149
20. Woodworth G, McGirt MJ, Samdani A, Garonzik I, Olivi A, Weingart JD (2005) Accuracy of frameless and frame-based image-guided stereotactic brain biopsy in the diagnosis of glioma: comparison of biopsy and open resection specimen. Neurol Res 27:358–362
21. Woodworth GF, McGirt MJ, Samdani A, Garonzik I, Olivi A, Weingart JD (2006) Frameless image-guided stereotactic brain biopsy procedure: diagnostic yield, surgical morbidity, and comparison with the frame-based technique. J Neurosurg 104:233–237
22. Yamaguchi F, Takahashi H, Teramoto A (2007) Photodiagnosis for frameless stereotactic biopsy of brain tumor. Photodiagn Photodyn Ther 4:71–75
23. Grunert P, Espinosa J, Busert C et al (2002) Stereotactic biopsied guided by an optical navigation system: technique and clinical experience. Minim Invasive Neurosurg 45:11–15
24. Waters JD, Gonda DD, Reddy H, Kasper EM, Warnke PC, Chen CC (2013) Diagnostic yield of stereotactic needle-biopsies of subcubic centimeter intracranial lesions. Surg Neurol Int 4:S176–S181
25. Krieqer MD, Chandrasoma PT, Zee CS, Apuzzo ML (1998) Role of stereotactic biopsy in the diagnosis and management of brain tumors. Semin Surg Oncol 14:13–25
26. Smith JS, Quinones-Hinojosa A, Barbaro NM, McDermott MW (2005) Frame-based stereotactic biopsy remains an important diagnostic tool with distinct advantages over frameless streotatic biopsy. J Neurooncol 73:173–179
27. Gempt J, Buchmann N, Ryang YM et al (2012) Frameless image-guided stereotaxy with real-time visual feedback for brain biopsy. Acta Neurochir (Wien) 154:1663–1667
28. Dammers R, Haitsma IK, Schouten KJM, Avezaat CJ, Vincent AJ (2008) Safety and efficacy of frameless and frame-based intracranial biopsy techniques. Acta Neurochir (Wien) 150:23–29
29. Frati A, Pichierri A, Bastianello S et al (2011) Frameless stereotactic cerebral biopsy: our experience in 296 cases. Stereotact Funct Neurosurg 89:234–245
30. Khatab S, Spliet W, Woerdeman PA (2014) Frameless image-guided stereotactic brain biopsies: emphasis on diagnostic yield. Acta Neurochir (Wien) 156:1441–1450